Letters

Analysis and Implementation of Parallel Connected Two-Induction Motor Single-Inverter Drive by Direct Vector Control for Industrial Application

Ramachandiran Gunabalan, *Member, IEEE*, Padmanaban Sanjeevikumar, *Senior Member, IEEE*, Frede Blaabjerg, *Fellow, IEEE*, Olorunfemi Ojo, *Fellow, IEEE*, and Veerana Subbiah, *Senior Member, IEEE*

***Abstract*—Sensorless-based direct vector control techniques are widely used for three-phase induction motor drive, whereas in case of multiple-motor control, it becomes intensively complicated and very few research articles in support to industrial applications were found. A straight-forward direct vector control with sensorless operation for parallel connected two similar-rated induction motors driven by single three-phase inverter is proposed and verified numerically by simulation software test under balanced and unbalanced conditions. The proposed control algorithm adapts the natural observer to estimate the rotor speed, rotor flux, and load torque of both motors. Simulation results along with theoretical background provided in this paper confirm the feasibility of operation of the ac motors and proves reliability for industrial applications.**

***Index Terms*—Estimator, field oriented control, induction motor, natural observer, sensorless vector control, speed control.**

I. Introduction

SENORLESS direct vector control (DVC) is widely applied for ac motor traction applications. On the availability information of line voltages and currents, speed can be estimated, but its accuracy is mostly meant for single inverter driven single-induction motor. In case of multiple-induction motors, control becomes a tough solution to handle with single inverter-based DVC. In point of reducing the cost, size, and to ensure less maintenance, a single-inverter driven multiple-induction motors in parallel combination is used for electric traction. In such cases, speed of the machines will be the same, if they have the same torque-speed characteristics and torque-sharing rates are equal in all operating conditions. But practically, two machines have observable differences in characteristics and the speeds may not be the same because of slight difference of wheel diameters.

In practice, both dissimilar machine characteristics and unequal wheel diameter problems exist. The machines speed-torque characteristics are shown in Fig. 1(a) for motors 1 and 2, and this causes the different torque sharing at the same speed. For instance, if the wheel diameter of machine 1 is a bit larger than that of machine 2 (assumed), then the torque sharing of machine 1 will be higher in motoring mode but lower in braking mode, where the corresponding characteristic is represented in Fig. 1(a). Now, the speed–torque behavior of both motors differs and unbalance condition arises (motors 1 and 2), the speeds of both motors deviate much from the command speed. Usually, in order to reduce these speed variations, average and differential currents are used to determine the reference currents [1]–[4].

Moreover, these above literatures dealt with speed sensorless drives, the estimation of speed and rotor fluxes were employed by the adaptive observers. The selection of gain matrix constant k is a tedious task in adaptive observers where the typical value of k is taken as 0.5. It is mandatory to have correction factors to track speed variations that results in the estimation lag actually with command signal. To overcome the above mentioned difficulties, a natural observer is used for estimations [5]. This paper proposes a sensorless DVC algorithm performed based on the natural observer and the complete scheme is verified by numerical simulation implementation.

II. Speed Estimation Using Natural Observer

Natural observer is actually an estimator, its structure and characteristic are identical to the induction motor, typically illustrated by Fig. 1(b). On looking at the convergence rate, the observer is faster than the motor in reaching the steady state, the equation for speed estimation is given below [5]:

$$\hat{T}_L = K_D e_P + K_P e_P + K_I \int_P^e \mathrm{dt} \,\text{limiting}\, \hat{T}_L \in (T_{\min}, T_{\max}) \tag{1}$$

where

$$e_P = V_{\mathrm{ds}}^s \left(\hat{i}_{\mathrm{ds}}^e - i_{\mathrm{ds}}^e\right) + V_{qs}^s \left(\hat{i}_{qs}^e - i_{qs}^e\right). \tag{2}$$

Estimation of rotor speed can be obtained from estimated stator current, rotor flux, and the estimated load torque as

$$\dot{\hat{\omega}}_r = \left(\frac{3}{2}\right)\left(\frac{n_p}{J}\right)\left(\frac{L_m}{L_r}\right)\left[\hat{\varphi}_{\mathrm{dr}}^s \hat{i}_{qs}^s - \hat{\varphi}_{qr}^s \hat{i}_{\mathrm{ds}}^s\right] - \frac{\hat{T}_L}{J} \tag{3}$$

Manuscript received January 28, 2015; revised April 10, 2015; accepted April 30, 2015. Date of publication May 8, 2015; date of current version August 21, 2015.

R. Gunabalan is with the School of Electrical Engineering, VIT University, Chennai 632014, India (e-mail: gunabalanr@yahoo.co.in).

P. Sanjeevikumar is with the Research and Development, Ohm Technologies, Chennai 632014, India (e-mail: sanjeevi_12@yahoo.co.in).

F. Blaabjerg is with the Department of Energy Technology, Aalborg University, Aalborg 9100, Denmark (e-mail: fbl@et.aau.dk).

O. Ojo is with the Department of Electrical and Computer Engineering, Tennessee Technical University, Cookeville, TN 38505 USA, and also with the Eskom Centre of Excellence in HVDC Engineering, University of KwaZulu-Natal, Durban 4001, South Africa (e-mail: Jojo@tntech.edu).

V. Subbiah is with the Department of Electrical and Electronics Engineering, PSG College of Technology, Coimbatore 641004, India (e-mail: subbiah42@yahoo.com).

Color versions of one or more of the figures in this paper are available online at http://ieeexplore.ieee.org.

Digital Object Identifier 10.1109/TPEL.2015.2429591

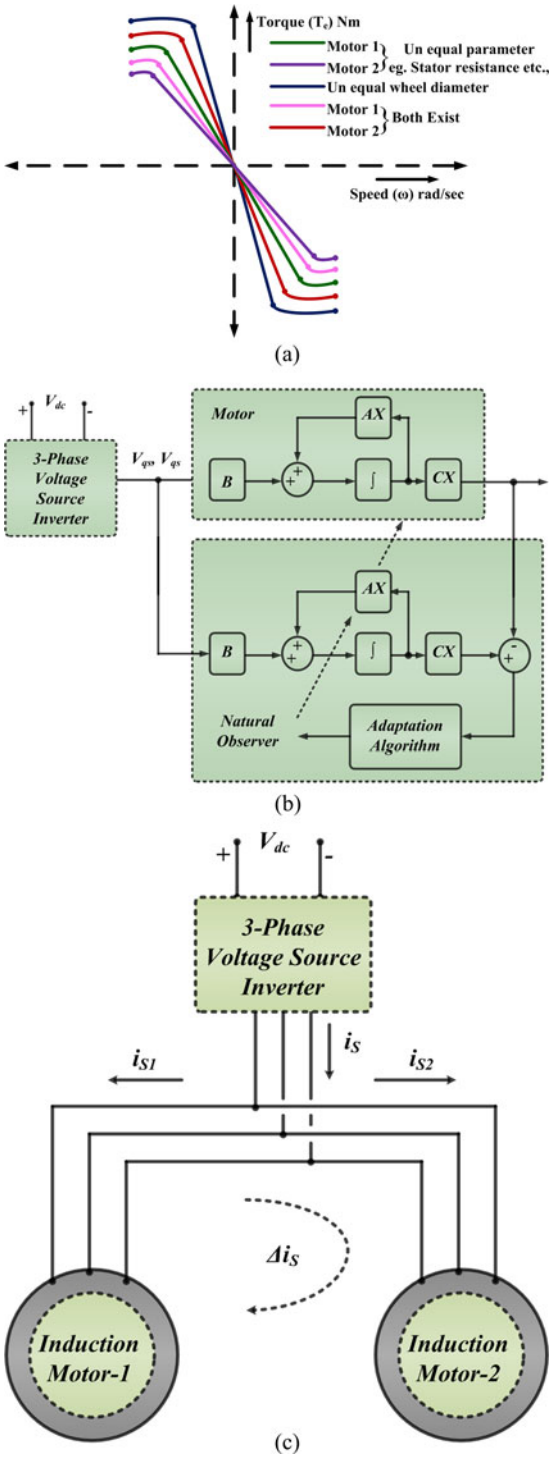

Fig. 1. (a) Speed-Torque characteristics of parallel-connected IM drives, (b) Block diagram of a natural observer, (c) Configuration of parallel-connected induction motor drives.

where n_p is the number of pole pairs and J is inertia of motor load system (kg·m^2).

Parallel connected two induction motors fed by single-inverter drive are shown in Fig. 1(c).

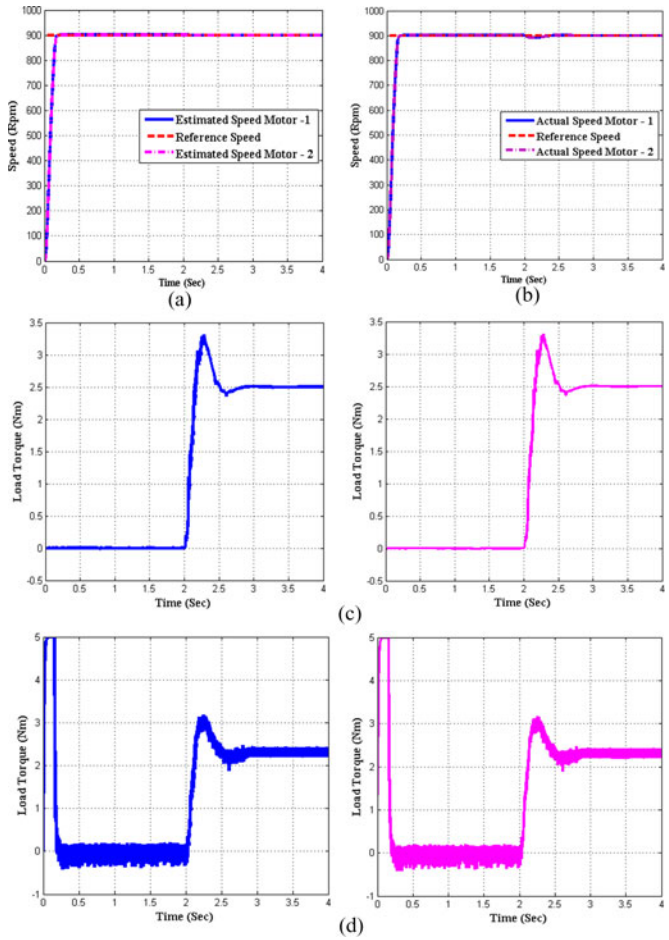

Fig. 2. Simulation results for balanced load conditions.(a) Estimated speed response. (b) Actual speed response. (c) Estimated load torque response. (Left-Motor 1, Right-Motor 2). (d) Axtual load torque response. (Left-Motor 1, Right-Motor 2)

III. Numerical Simulation Test Verification and Results

Two identical 745.6 W, 3 Φ, 415 V, 1.8 A, 50 Hz, 4 pole, and 1415 r/min squirrel cage induction motors are used for testing. In balanced conditions, the two induction motors run at a reference speed of 900 r/min. At $t = 2$ s, a load of 2.5 N·m is applied to both induction motors. The estimated and actual speed waveforms are depicted in Fig. 2(a) and (b). Both motors follow the speed command. There is a slight dip in the actual speed at the time of applying sudden load that is negligible in the estimated speed. At steady state, the speed difference between the induction motors is zero. The estimated and actual load torque responses are shown by Fig. 2(c) and (d). The estimated speeds match the speed command and the estimated torque of both induction motors follows the load torque.

To illustrate unbalanced load condition (dissimilar wheel diameter), both induction motors run at a constant speed of 900 r/min. A load of 2.5 N·m is applied to motor 2 and motor 1 is at no load condition at $t = 2$ s. Now, the wheel diameter of motor 2 is larger than motor 1 and the torque of motor 2 is greater than motor 1. The estimated and actual speeds of both motors are

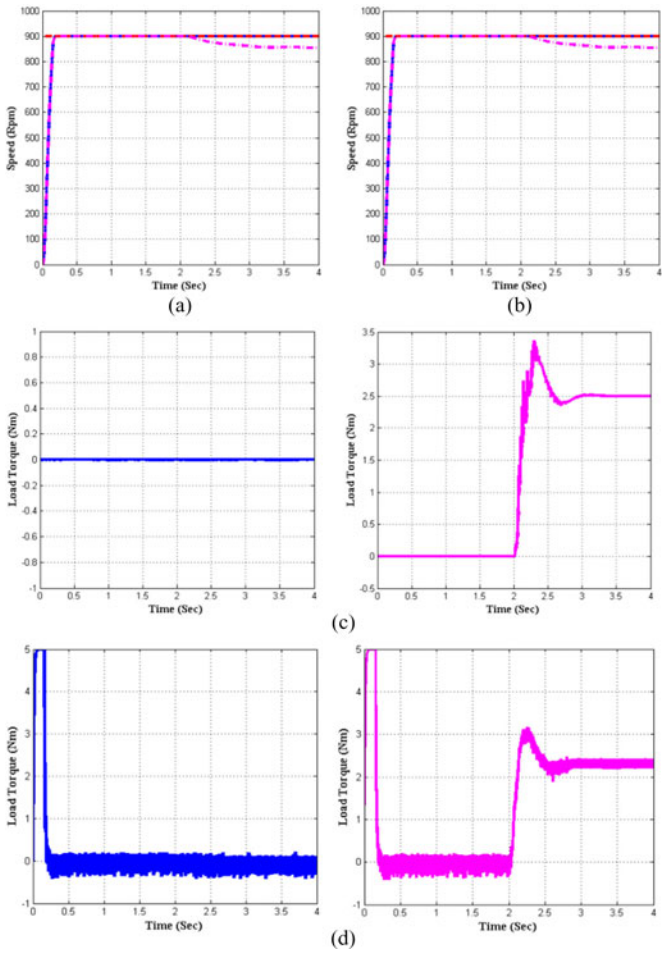

Fig. 3. Simulation results for unbalanced load conditions. (a) Estimated speed response. (b) Actual speed response. (c) Estimated load torque response. (Left-Motor 1, Right-Motor 2). (d) Axtual load torque response. (Left-Motor 1, Right-Motor 2)

given in Fig. 3(a) and (b). It is observed that the speed of motor 2 decreases to 880 r/min and speed of motor 1 is maintained constant. With respect to the reference speed, the speed of motor 2 deviates by 20 r/min (2.22%), but however both motors run at steady speed makes system stable condition. The estimated and actual torque responses of both motors are shown by Fig. 3(c) and (d).

Stator resistance plays an important role in low-speed operation and its value has to be known with good precision in order to obtain an accurate estimation of the rotor speed. To accommodate the change in parameter, the stator resistance of motor 2 is increased to 50% ($R_{s2} = 20.025\,\Omega$) and the parameters of motor 1 remain the same. Speed command is set at 1000 r/min. Both the motors are initially at no load condition and at $t = 2$ s, a balanced load of 2.5 N·m is applied to both motors. Fig. 4(a) and (b) shows the estimated and actual speed responses of motor 1 and 2 for variations in stator resistances. The speed difference arises because of difference in stator resistances of motors 1 and 2.

Further, dc supply voltage (100–50–100)% large-step variation test is conducted to verify the performance of the parallel

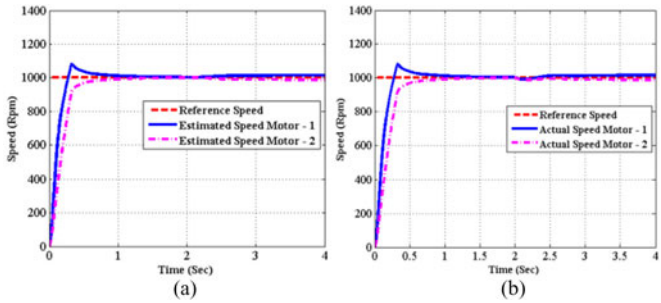

Fig. 4. Simulation results for unbalanced stator resistance between motors 1 and 2. (a) Estimated speed response. (b) Actual speed response.

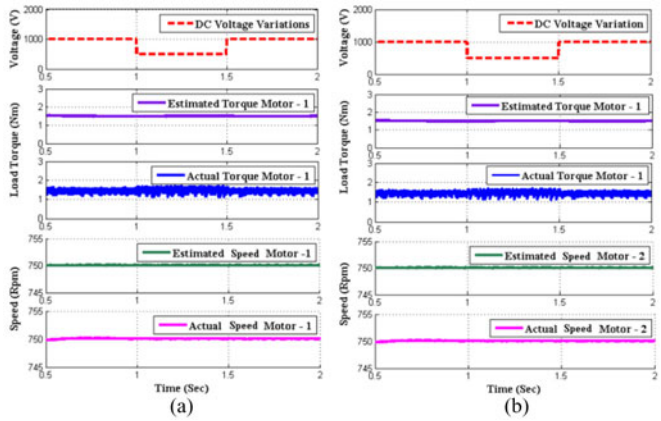

Fig. 5. Simulation results for large-step variation of dc voltage variations. (a) Resplonse of Motor 1. (b) Response of Motor 2.

connected two motors in fluctuating dc supply drooping conditions. To conduct this test in safe and to avoid saturation of three-phase inverter power demands, the speed and torque are reduced to 750 r/min and 1.5 N·m. Fig. 5(a) from top-to-bottom shows the obtained numerical simulation performances, the DC supply voltage variation from between 1000 V and 500 V in every 0.5 sec, the estimated and actual torque, and speed for motor 1. Similarly for the motor 2, it is shown in Fig. 5(b) and results confirm that under dc supply drooping conditions, the speed and torque of the parallel connected two motors follow the set conditions with smooth propagation of torque and speed at 750 r/min and 1.5 N·m.

Finally, efficiency and copper loss of the two-motor drive system are numerically calculated by the simulation test conducted at different operating speed with constant torque ($T = 2.5$ N·m) conditions and includes the field weakening region (speed above rated and torque at 2.5 N·m). Efficiency of ac motors are shown in Fig. 6, motor 1 (first bar-speed, second bar-efficiency from reference to x-axis) and motor 2 (third bar-speed, fourth bar-efficiency from reference to x-axis). Correspondingly, Fig. 7 shows the stator current and copper losses of the two motors at different operating speed conditions. It is confirmed that both motors have the same efficiency and losses at different speeds with constant torque including the field weakening region. From the results, it is clear that the motors have poor

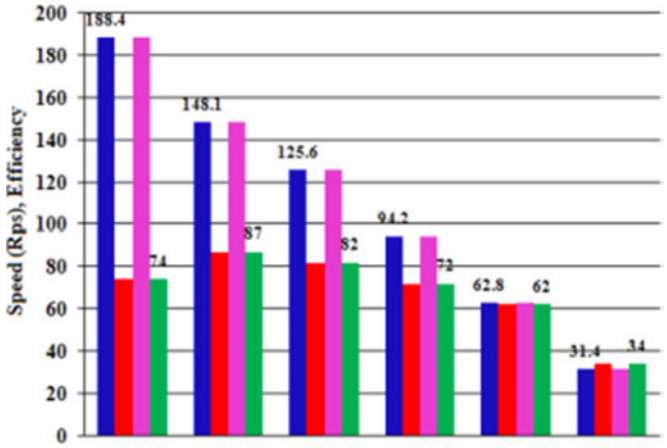

Fig. 6. Numerically calculated efficiency of the parallel connected motors at different operating speed condition includes field weakening region (torque $\mathrm{T} = 2.5$ Nm kept constant). Motor 1 (first bar-speed, second bar-efficiency), Motor 2 (third bar-speed, fourth bar-efficiency) in reference to Y-axis.

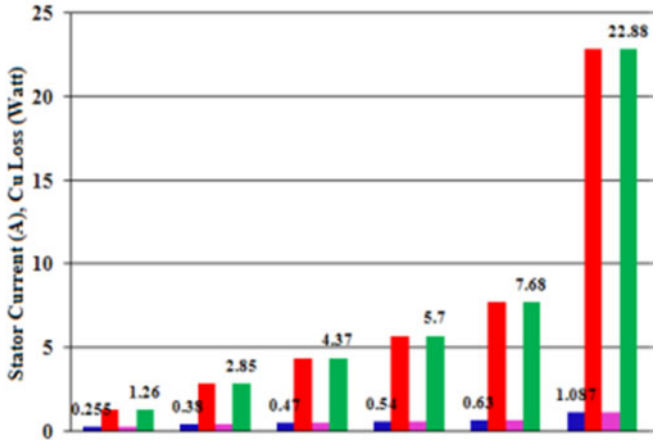

Fig. 7. Numerically calculated stator currents and copper losses of the parallel connected motors at different operating speed condition includes field weakening region (torque $\mathrm{T} = 2.5$ Nm kept constant). Motor 1 (first bar-stator current, second bar-cu loss), Motor 2 (third bar-stator current, fourth bar-cu loss) in reference to Y-axis.

efficiency and comparatively high-copper losses at lower operating speed ranges in comparison to variations near to rated speed and field-weakening region.

IV. Conclusion

This paper provides a straightforward approach for DVC with sensorless operation for two motors connected in parallel and fed by a single inverter. Natural observer with load torque adaption technique is used to estimate the speed and torque of the motors. By numerical simulation test, it is confirmed that the complete system is stable under balanced and unbalanced load conditions. Also, concluded that the performance of torque tracking and speed control are apparently better than conventional method proposed in the literatures. The proposed concept can be easily implemented by industrial DSPs.

References

[1] F. Xu, L. Shi, and Y. Li, "The weighted vector control of speed-irrelevant dual induction motors fed by the single inverter," *IEEE Trans. Power Electron.*, vol. 28, no. 12, pp. 5665–5672, Dec. 2013.

[2] A. Kazuya, Y. Takahashi, K. Matsuse, S. Ito, and Y. Nakajima, "Speed characteristics of sensorless vector controlled two unbalanced induction motor drive fed by single inverter," presented at the 15th Int. Conf. Elect. Mach. Syst., Sapporo, Japan, 2012.

[3] T. Inoue, K. Azegami, K. Matsuse, S. Ito, and Y. Nakajima, "Dynamic performance of sensorless vector controlled multiple induction motor drive connected in parallel fed by inverter (single)," presented at the Ind. Appl. Soc. Meet., Orlando, FL, USA, Oct. 2011.

[4] K. Matsuse, Y. Kouno, H. Kawai, and J. Oikawa, "Characteristics of speed sensorless vector controlled dual induction motor drive connected in parallel fed by a single inverter," *IEEE Trans. Ind. Appl.*, vol. 40, no. 1, pp. 153–161, Jan./Feb. 2004.

[5] R. Sidney Bowes, A. Sevinc, and D. Holliday, "New natural observer applied to speed sensorless dc servo and induction motors," *IEEE Trans. Ind. Appl.*, vol. 51, no. 5, pp. 1025–1032, Oct. 2004.